Morphological and elemental analysis of space launch vehicle debris retrieved from a Philippine coastal area

Danielle Camille P. Canillo,*[1] Toni Beth G. Lopez,[1,2] Dominic P. Guaña,[1] Paul Leonard Atchong C. Hilario,[1] Manuel R. del Rosario, Jr.,[1] Gil Nonato C. Santos,[2] and Gay Jane P. Perez[1,3]

[1]*Philippine Space Agency, Eastwood Avenue, Quezon City*
[2]*De La Salle University, Taft Avenue, Manila*
[3]*Institute of Environment Science and Meteorology, University of the Philippines Diliman, Quezon City*
*Corresponding author: danielle.canillo@philsa.gov.ph

Abstract

Payload fairing debris retrieved post-launch within Philippine territorial waters was subjected to morphology and elemental analysis using Scanning Electron Microscopy and Energy Dispersive X-ray Spectroscopy (SEM-EDS). Cracks and deformations, which may have been incurred from the launch, are present on the surface of most samples. Identified elements provides hints on the purpose of the parts recovered from the debris.

Keywords: surface morphology, elemental analysis, payload fairing

1 Introduction

The growing demand for space exploration has led to the advancement of space technology. New Space is marked by commercialization of space activities [1] which results in an increase in the number of launches due to improved accessibility and affordability during launch cost. While they bring the benefits from space to a wider range of people and to more nations, the increase in space vehicle launches (SVLs) contribute to the addition in debris which may pose risks to life, property, and environment, as rocket parts may impact on these objects after jettison during ascent. Another possibility is the presence of toxic chemicals from fuel residues and paint, and heavy metals and other reactive components present to ensure compliance to requirements in basic mass, damage tolerance during use, sensitivity to fabrication defects, acoustic transmissibility, thermal tolerance, environmental sensitivity, and cost-savings [2-3]. The presence of these compounds may pose problems as the debris are first found by fisherfolks and are recovered by the first respondents by hand.

Testing the materials used in space launch vehicles is routinely performed to determine the presence or absence of potentially risky substances. In this paper, scanning electron microscopy (SEM) is coupled with energy-dispersive X-ray spectroscopy (EDS) to help understand the relationship between the elemental composition and microstructure of the samples taken from a recovered SLV debris. SEM provided information on the surface morphology while EDS was used to detect and analyze the X-ray emittance spectrum of elements presents in a sample [5]. In this study, the morphology and elemental composition of various components of space launch vehicle debris was investigated.

2 Debris retrieval and measurement

The PhilSA Launch Vehicle Debris Examination team has confirmed the identity of the debris as part of a module launch. Prior to the launch, a Notice to Airmen (NOTAM) warning was released by the Civil Aviation Authority of the Philippines (CAAP), indicating two drop zones in the Philippines. Nine days after the launch, the payload fairing debris which still bore the markings of the module, was recovered in a particular coastal area. The length was measured using a laser rangefinder. Measurements of the chord length and height of the debris were both taken using a tape measure, while the measurements of the inner and outer shell and the honeycomb structure were taken using a vernier caliper. Samples from the paint, washer screw, adhesive, and honeycomb panel were obtained and stored in pouch bags for further analysis.

A reconstruction of the payload fairing debris with measurements is seen in Fig. 1a. The payload fairing debris/panel measures about 4.373 ± 0.001 m in its long dimension while the chord length is about 2.077 ± 0.001 m on one side. The height or the rise of the debris is about 0.246 ± 0.001 m. Close up inspection of the outer shell/cladding revealed signs of oxidation, discoloration, and structural deformation possibly due to burning -

either during ascent, descent, or ejection on drop zone (Fig. 1b). The inner shell/cladding is a metal finish with various cone point set screws and flat washers. It must be noted that the debris/panel is not made of purely solid metal but rather layers of different materials in varied configurations. The outer cladding/shell is a 1.93 ± 0.05 mm thin sheet of painted metal with cardboard padding beneath it (Fig. 1d). The padding is glued to a 26.31 ± 0.05 mm high metal honeycomb structure opened in both ends. It is then further glued to the 0.63 ± 0.05 mm thick inner metal cladding/shell. The probable reasoning for this design could be to promote a durable but lightweight payload fairing suitable for launch vehicles.

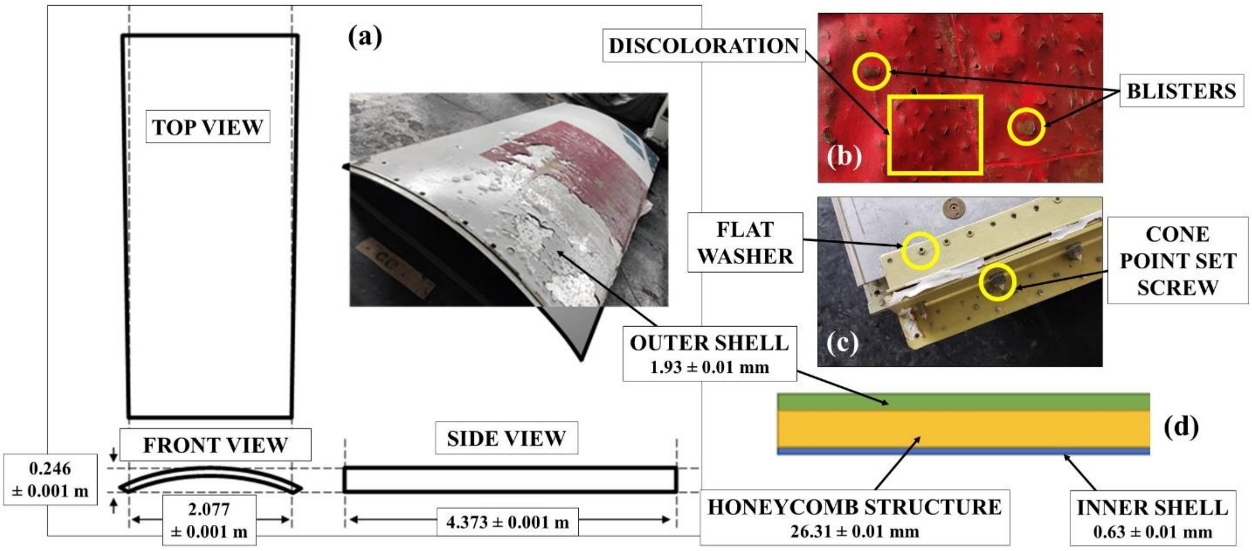

Figure 1. (a) Reconstruction of the payload fairing debris. (b) Discoloration and blisters on the outer shell possibly due to burning. (c) Screws (d) The cross-section measurements of honeycomb sandwich panel.

3 Results and discussion

SEM images of portions with minimum size of *5 mm* up to maximum size of *10 mm* obtained from the SLV debris were obtained using Phenom Pro desktop scanning electron microscope (Phenom-World, Eindhoven, Netherlands) operating at an acceleration voltage of *15kV*. Elemental analysis was carried out using Phenom ProSuite software energy-dispersive X-ray spectroscopy (Phenom-World, Eindhoven, Netherlands) with the same acceleration voltage. A thin layer of gold was applied using a JFC 1200 fine coater (JEOL Ltd., Tokyo, Japan) prior to the analysis to improve the image quality.

Emission spectra of the honeycomb panels (Figures 2 - 3) reveal that they are aluminum-based. The high concentration of oxygen possibly suggests the presence of aluminum oxide, which is used in aerospace and space launch vehicles due to its mechanical strength, low thermal conductivity, and high corrosion and electrical resistance [6-7]. Alumina ceramic fibers are also used for providing structural and thermal insulation, as well as for reinforcing materials by being dispersed within composite systems consisting of metals, ceramics, or polymers [8-9]. Surface analysis revealed cracks and globular-like protrusion on the material. While the actual cause of these structures merit additional research, it is noteworthy that launch and jettison generate stresses that may result to cracks and protrusions.

Paint was also recovered on the debris surface. The paint surface morphology shows a mostly smooth surface with aggregates almost equally distributed. Rectangular microstructures as well as big cracks are seen in the high magnification images as shown in Figure 4. The elemental composition of the paint sample comprises mostly of carbon and oxygen with considerable amount of niobium which is commonly used in anti-corrosion paints. SEM images and emission spectrum of the cardboard padding are shown in Figure 5. shows hollow, hexagonal-like microstructures making the padding porous. This hints on the function of the padding to dampen the sound waves produced during launch. Emission spectrum shows that the padding is mostly carbon and oxygen with some hints of magnesium and bromine, which hints on the use of magnesium bromide commonly used as flame retardant.

Figures 6 shows that the sealant used in the debris is silicone-based, which is known for its adhesive properties. Lastly, the images of the washer screw (Figure 7) show rough morphology across the different magnifications. The presence of carbon and zinc hints that stainless steel is used on washer screw.

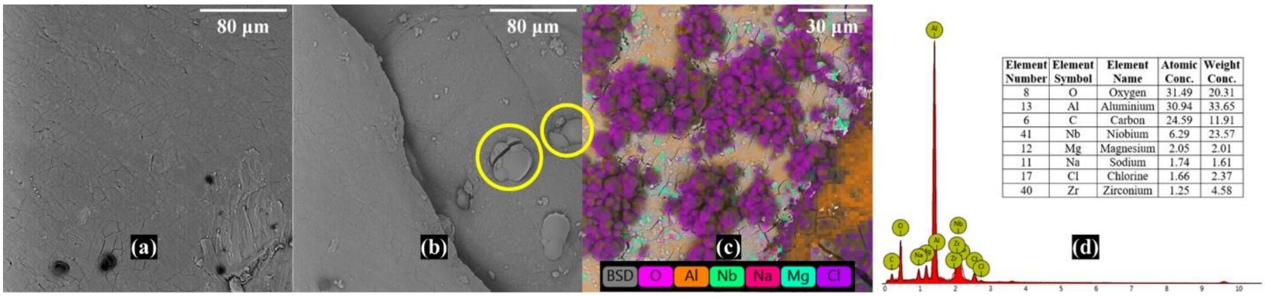

Element Number	Element Symbol	Element Name	Atomic Conc.	Weight Conc.
8	O	Oxygen	31.49	20.31
13	Al	Aluminium	30.94	33.65
6	C	Carbon	24.59	11.91
41	Nb	Niobium	6.29	23.57
12	Mg	Magnesium	2.05	2.01
11	Na	Sodium	1.74	1.61
17	Cl	Chlorine	1.66	2.37
40	Zr	Zirconium	1.25	4.58

Figure 2. Inverted honeycomb portion of the debris at (a-b) 1000x magnification. A representative image was used to generate the (c) combined elemental map and the (d) elemental spectrum of the sample.

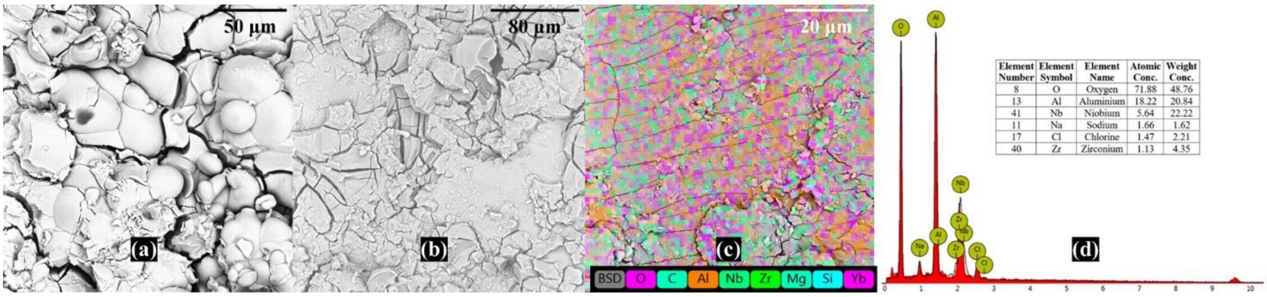

Element Number	Element Symbol	Element Name	Atomic Conc.	Weight Conc.
8	O	Oxygen	71.88	48.76
13	Al	Aluminium	18.22	20.84
41	Nb	Niobium	5.64	22.22
11	Na	Sodium	1.66	1.62
17	Cl	Chlorine	1.47	2.21
40	Zr	Zirconium	1.13	4.35

Figure 3. Honeycomb panel of the debris at (a) 1350x and (b) 1000x magnifications. A representative image was used to generate the (c) combined elemental map and the (d) elemental spectrum of the sample.

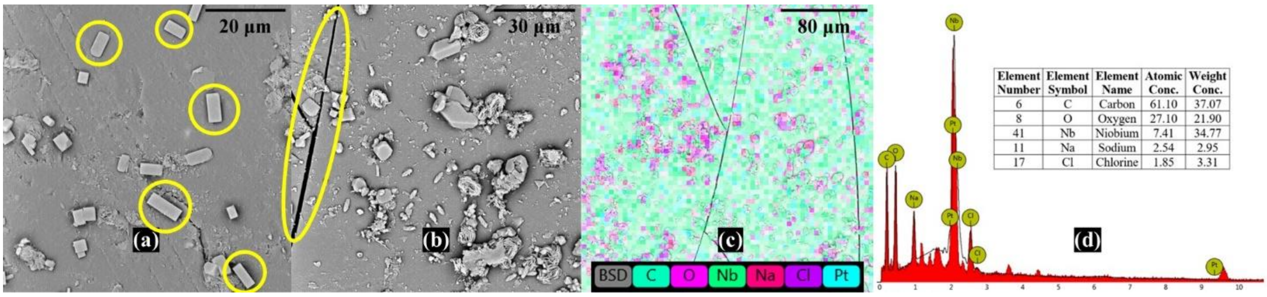

Element Number	Element Symbol	Element Name	Atomic Conc.	Weight Conc.
6	C	Carbon	61.10	37.07
8	O	Oxygen	27.10	21.90
41	Nb	Niobium	7.41	34.77
11	Na	Sodium	2.54	2.95
17	Cl	Chlorine	1.85	3.31

Figure 4. Paint chip at (a) 3700x and (b) 2500x magnifications. A representative image was used to generate the (c) combined elemental map and the (d) elemental spectrum of the sample.

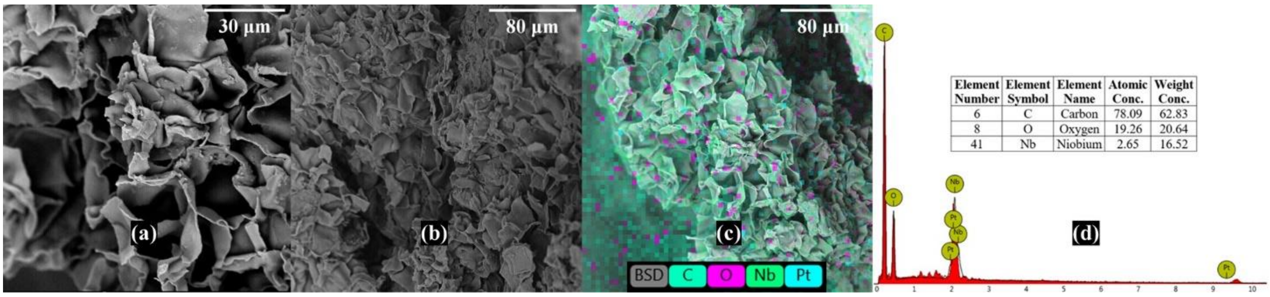

Element Number	Element Symbol	Element Name	Atomic Conc.	Weight Conc.
6	C	Carbon	78.09	62.83
8	O	Oxygen	19.26	20.64
41	Nb	Niobium	2.65	16.52

Figure 5. Acoustic panel at (a) 350x and (b) 1000x magnifications. A representative image was used to generate the (c) combined elemental map and the (d) elemental spectrum of the sample.

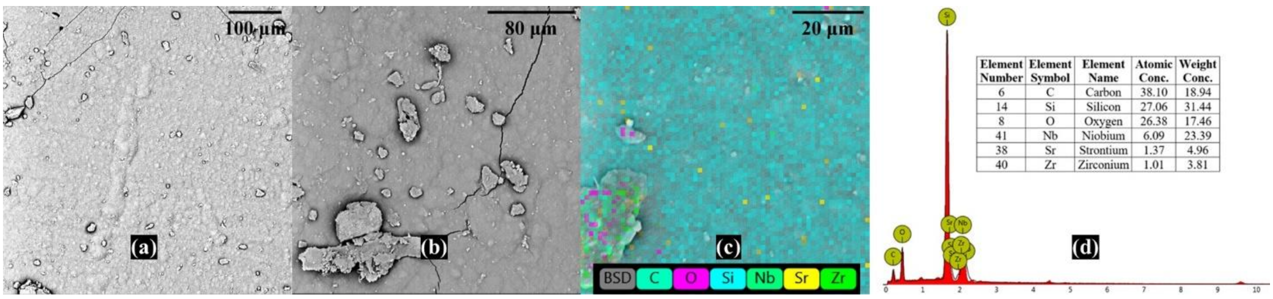

Element Number	Element Symbol	Element Name	Atomic Conc.	Weight Conc.
6	C	Carbon	38.10	18.94
14	Si	Silicon	27.06	31.44
8	O	Oxygen	26.38	17.46
41	Nb	Niobium	6.09	23.39
38	Sr	Strontium	1.37	4.96
40	Zr	Zirconium	1.01	3.81

Figure 6. Adhesive at (a) 500x and (b) 1000x magnifications. A representative image was used to generate the (c) combined elemental map and the (d) elemental spectrum of the sample.

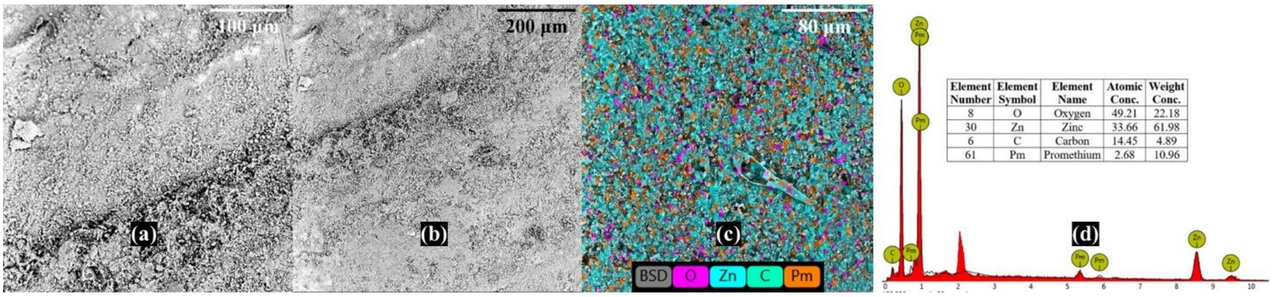

Figure 7. Washer screw at (a) 710x and (b) 360x magnifications. A representative image was used to generate the (c) combined elemental map and the (d) elemental spectrum of the sample.

4 Conclusions

The morphology and the elemental composition of the payload fairing debris was analyzed using SEM-EDX. Morphologies of the parts showed rough surface and cracks, although these could not be validated as an intrinsic property of the materials, or as damage induced by the launch. The qualitative and quantitative determination of elements gives a significant insight into the purpose of a material and how it reacts with other elements. We were also not able to detect toxic elements beyond the limits of detection of the equipment. While this is the case for the particular debris, the composition and conditions for other debris, specially from a different launch technology may not be identical, hence, future researchers is still advised to practice caution in retrieving and handling of unknown debris.

Acknowledgements

The launch vehicle debris was retrieved by the Philippine Coast Guard. Samples were collected by the members of the Philippine Space Agency Launch Vehicle Debris Examination Team. Lastly, the tests were performed at the iNano Research Facility of De La Salle University, Malate, Manila, for the use of equipment.

References

[1] M. Weinzierl, Space, the final economic frontier, *J. Econ. Persp*. **32**, 173 (2018). URL: https://doi.org/10.1257/jep.32.2.173

[2] M. Krivanek and B.C. Yount, *Composite Payload Fairing Structural Architecture Assessment and Selection*, Technical Report E-18094, (NASA Technical Reports Server, 2012). URL: https://ntrs.nasa.gov/citations/20120009204

[3] Z. Wang, Recent advances in novel metallic honeycomb structure, *Compos. B. Eng*. **166**, 731 (2019). URL: https://doi.org/10.1016/j.compositesb.2019.02.011

[4] B. Hafner, Scanning electron microscopy primer (2007), retrieved from http://www.charfac.umn.edu/instruments/sem_primer.pdf.

[5] M. Scimeca, A. Orlandi, I. Terrenao, S. Bischetti, and E. Bonnano, Assessment of metal contaminants in non-small cell lung cancer by EDX microanalysis, *Eur. J. Histochem.* **58**, 2403 (2014). URL: https://doi.org/10.4081/ejh.2014.2403

[6] C. Han, H. Li, H. Pu, H. Yu, L. Deng, S. Huang, and Y. Luo, Synthesis and characterization of mesoporous alumina and their performances for removing arsenic(V), *Chem. Eng. J.* **217**, 1 (2013). URL: https://doi.org/10.1016/j.cej.2012.11.087

[7] B. Clauss, and D. Schawaller, Modern aspect of ceramic fiber development, *Adv. Sci. Technol*. **50**, 1 (2006). URL: https://doi.org/10.4028/www.scientific.net/AST.50.1

[8] A. Sedaghat, E. Taheri-Nassaj, and R. Naghizadeh, An alumina mat with a nano microstructure prepared by centrifugal spinning method, *J. Non-Cryst. Solids.* **352**, 2818 (2006). URL: https://doi.org/10.1016/j.jnoncrysol.2006.02.068

[9] R. Venkatesh, P. K. Chakrabarty, B. Siladitya, M. Chatterjee, D. Ganguli, Preparation of alumina fibre mats by a sol-gel spinning technique, *Ceram. Int.* **25**, 539 (1999). URL: https://doi.org/10.1016/S0272-8842(97)00092-8